HHS Public Access
Author manuscript
Ear Hear. Author manuscript; available in PMC 2021 August 31.

Published in final edited form as:
Ear Hear. 2020 ; 41(5): 1349–1361. doi:10.1097/AUD.0000000000000864.

Frequency-to-Place Mismatch: Characterizing Variability and the Influence on Speech Perception Outcomes in Cochlear Implant Recipients

Michael W. Canfarotta, MD, **Margaret T. Dillon, AuD**, **Emily Buss, PhD**, **Harold C. Pillsbury, MD**, **Kevin D. Brown, MD, PhD**, **Brendan P. O'Connell, MD**
Department of Otolaryngology/Head and Neck Surgery, University of North Carolina at Chapel Hill, NC

Abstract

Objectives: The spatial position of a cochlear implant (CI) electrode array affects the spectral cues provided to the recipient. Differences in cochlear size and array length lead to substantial variability in angular insertion depth (AID) across and within array types. For CI-alone users, the variability in AID results in varying degrees of frequency-to-place mismatch between the default electric frequency filters and cochlear place of stimulation. For electric-acoustic stimulation (EAS) users, default electric frequency filters also vary as a function of residual acoustic hearing in the implanted ear. The present report aimed to: 1) investigate variability in AID associated with lateral wall arrays, 2) determine the subsequent frequency-to-place mismatch for CI-alone and EAS users mapped with default frequency filters, and 3) examine the relationship between early speech perception for CI-alone users and two aspects of electrode position: frequency-to-place mismatch and angular separation between neighboring contacts, a metric associated with spectral selectivity at the periphery.

Design: One hundred one adult CI recipients (111 ears) with MED-EL Flex24 (24 mm), Flex28 (28 mm), and FlexSOFT/Standard (31.5 mm) arrays underwent postoperative computed tomography to determine AID. A subsequent comparison was made between AID, predicted spiral ganglion place frequencies, and the default frequency filters for CI-alone (n = 84) and EAS users (n = 27). For CI-alone users with complete insertions who listened with maps fit with the default frequency filters (n = 48), frequency-to-place mismatch was quantified at 1500 Hz and angular separation between neighboring contacts was determined for electrodes in the 1-2 kHz region. Multiple linear regression was used to examine how frequency-to-place mismatch and angular separation of contacts influence consonant-nucleus-consonant (CNC) scores through 6 months post-activation.

Results: For CI recipients with complete insertions (n = 106, 95.5%), the AID (mean ± standard deviation) of the most apical contact was 428° ± 34.3° for Flex24 (n = 11), 558° ± 65.4°

Corresponding Author: Michael W. Canfarotta, MD, Department of Otolaryngology/Head & Neck Surgery, 170 Manning Drive, CB 7070, Physicians Office Building, Room G-190, Chapel Hill, NC 27599-7070, Phone: (919)966-3343 Fax: (919)966-7941, michael.canfarotta@unchealth.unc.edu.
Author Contributions:
MWC, MTD, EB and BPO designed experiments. Implanting surgeons were HCP, KDB and BPO. MWC, MTD, EB and BPO wrote the paper, and all authors contributed significantly to analysis and revisions leading to its final form.

for Flex28 (n = 48), and 636° ± 42.9° for FlexSOFT/Standard (n = 47) arrays. For CI-alone users, default frequency filters aligned closely with the spiral ganglion map for deeply inserted lateral wall arrays. For EAS users, default frequency filters produced a range of mismatches; absolute deviations of ≤ 6 semitones occurred in only 37% of cases. Participants with shallow insertions and minimal or no residual hearing experienced the greatest mismatch. For CI-alone users, both smaller frequency-to-place mismatch and greater angular separation between contacts were associated with better CNC scores during the initial 6 months of device use.

Conclusions: There is significant variability in frequency-to-place mismatch among CI-alone and EAS users with default frequency filters, even between individuals implanted with the same array. When using default frequency filters, mismatch can be minimized with longer lateral wall arrays and insertion depths that meet the edge frequency associated with residual hearing for CI-alone and EAS users, respectively. Smaller degrees of frequency-to-place mismatch and decreased peripheral masking due to more widely spaced contacts may independently support better speech perception with longer lateral wall arrays in CI-alone users.

Introduction

The default mapping procedures for cochlear implant (CI) and electric-acoustic stimulation (EAS) devices capitalize on the tonotopic organization of the cochlea by distributing low-frequency information at the apical end of the electrode array and high-frequency information at the base. Electrode arrays vary in length across and within manufacturers (Dhanasingh & Jolly 2017), which may result in discrepancies between the distribution of frequency information and the natural tonotopic organization of the cochlea, known as a *frequency-to-place mismatch*. Adding further complexity, there are marked interindividual anatomic variations in cochlear size and cochlear duct length (Hardy 1938; Wurfel et al. 2014; Meng et al. 2016), leading to differences in angular insertion depth (AID) even within patient cohorts implanted with the same array. This may be of particular importance in postlingually deafened CI recipients, who are familiarized with a normal frequency-to-place function along the basilar membrane prior to hearing loss and must adapt to varying degrees of mismatch when listening with a CI-alone or EAS device.

Prior work has demonstrated a mismatch between the default frequency filters for individual electrode contacts and the associated spiral ganglion (SG) frequency estimate across several arrays in the CI-alone condition (Landsberger et al. 2015; Venail et al. 2015; Wess et al. 2017). While CI-alone users can learn to use frequency-shifted information, mismatch between the electric place of stimulation and the normal frequency-to-place function may prolong the acclimatization period and reduce asymptotic performance (Svirsky et al. 2004). Yet to date, the influence of this mismatch remains unclear, with several studies showing either no effect or a decrement in performance with greater depths of insertion (Gani et al. 2007; Finley et al. 2008; Lazard et al. 2012; Holden et al. 2013). With respect to lateral wall arrays, there are emerging data that consistently demonstrate deep insertions confer a benefit in speech perception in the CI-alone condition (Hochmair et al. 2003; Yukawa et al. 2004; Buchman et al. 2014; O'Connell et al. 2016; Buchner et al. 2017; Chakravorti et al. 2019).

There are several mechanisms that could account for an association between deeper array insertions and better audiologic outcomes. First, deep insertions extend the range of low-frequency pitch percepts (Prentiss et al. 2014; Schatzer et al. 2014; Vermeire et al. 2015; Dillon, Buss, et al. 2019), which may contribute to better speech perception in noise. Second, the default frequency filters for electrode contacts on deeply inserted arrays more closely align with the natural tonotopicity of the cochlea, allowing users to benefit from place and rate cues (Schatzer et al. 2014; Landsberger et al. 2018). It should be noted that frequency-to-place alignment is highly dependent on the specific frequency filters for individual electrode contacts, and this information has not typically been controlled in prior investigations. Lastly, the angular separation between neighboring electrode contacts differs across arrays and insertion depths, with larger angular separation for longer arrays and deeper insertions. This greater separation would tend to reduce peripheral masking and increase functional spectral resolution, which could result in better speech perception (Won et al. 2007; Zhou 2017). Thus, if one chooses to use a lateral wall array for a patient destined for a CI-alone device, there are reasons to prefer a longer array.

Selecting the optimal array length becomes more challenging for the growing population of patients with considerable residual hearing in the implanted ear. Cochlear implant recipients with preserved hearing are able to use EAS devices to gain substantial benefit with speech perception in noise and spatial hearing as compared to a CI or hearing aid alone (Gantz et al. 2009; Dunn et al. 2010; Helbig et al. 2011; Gifford & Dorman 2012; Gifford et al. 2013; 2014; Rader et al. 2013; Dillon et al. 2015; Pillsbury et al. 2018). It is widely accepted that shorter arrays that do not reach the apical region of the cochlea inflict less trauma and maximize chances of hearing preservation (Gantz et al. 2016; Suhling et al. 2016; O'Connell et al. 2017). However, in the event that residual hearing is lost, short array recipients using default frequency filters experience greater frequency-to-place mismatch and greater peripheral masking associated with distributing the full spectrum of speech cues on a short array. This results in poorer speech perception than observed for long array recipients (Buchner et al. 2017). Interestingly, hearing preservation has been demonstrated in recipients of longer flexible lateral wall arrays (Tamir et al. 2012; Mick et al. 2014; Usami et al. 2014; Moteki et al. 2018), which provide greater cochlear coverage for electric stimulation if acoustic hearing is lost. With emerging data that support the feasibility of hearing preservation with longer arrays, there is likely to be substantial variability in AID amongst recent EAS device users.

The frequency-to-place mismatch for EAS device users is influenced not only by variability in array AID, but also the default frequency filters for EAS devices, which differ considerably from CI-alone default settings. The default frequency filters for EAS devices use the patient's acoustic hearing thresholds in the implanted ear to determine the output of the acoustic component and the lowest frequency presented by the electric component, known as the *low-frequency cutoff* – without consideration of the AID. As such, variability in AID and amount of residual acoustic hearing between EAS users may result in significant variability in frequency-to-place mismatch unique to each recipient. Furthermore, if the recipient experiences a change in residual hearing after device activation, the default setting shifts the low-frequency cutoff, subsequently re-distributing frequency information logarithmically across the entire array. The change in electric frequency filters requires the patient to re-acclimate to new map settings, which could negatively affect early performance and may reduce asymptotic performance with the device. As outcomes have been shown to be variable amongst EAS users (Polak et al. 2010; Dillon et al. 2014; Gifford et al. 2017), it is possible that the need to adapt to varying degrees of frequency-to-place mismatch and peripheral masking may limit performance.

Given the possible role of frequency-to-place mismatch in outcomes for CI-alone and EAS device users, it is important to understand the range of mismatches obtained with different arrays and map settings. The primary aims of the current study were as follows: 1) investigate the variability in AID associated with Flex24, Flex28, and FlexSOFT/Standard arrays, 2) determine the associated frequency-to-place mismatch when CI-alone and EAS device users are mapped with default electric frequency filters, and 3) examine the relationship between early speech perception for CI-alone users and two aspects of electrode position: frequency-to-place mismatch and angular separation between neighboring contacts, a metric associated with spectral selectivity at the periphery.

Materials and Methods

Participants

Study procedures were approved by the Institutional Review Board, and participants provided consent to participate. Adult CI recipients presenting for routine follow-up implanted with MED-EL GmbH (Innsbruck, Austria) Flex24 (24 mm), Flex28 (28 mm), or FlexSOFT/Standard (31.5 mm) electrode arrays were eligible for inclusion. FlexSOFT and Standard array data were combined, as both designs have the same array length and distance between contacts. A postoperative high-resolution temporal bone cone-beam computed tomography (CT) scan was obtained in all cases. Participants with cochlear malformations were excluded from the study.

Participants were grouped as CI-alone or EAS device users by their unaided hearing thresholds in the implanted ear measured at device activation (approximately 2-4 weeks postoperatively). The MED-EL clinical software (MED-EL GmbH, Maestro, version 7) uses an unaided threshold of 65 dB HL to determine the low-frequency cutoff of electric stimulation. Considering this, participants with postoperative low-frequency hearing thresholds worse than 65 dB HL at 125 Hz were identified as CI-alone users, while participants with low-frequency hearing thresholds of better than or equal to 65 dB HL at 125 Hz were identified as EAS users.

Measurement of Angular Insertion Depth and Cochlear Duct Length

The postoperative CT was uploaded to OTOPLAN®, an otologic imaging analysis tool developed by CAScination AG (Bern, Switzerland) in collaboration with MED-EL GmbH, to calculate the AID for each electrode contact, as previously described (Canfarotta et al. 2019). Briefly, this algorithm uses the user-defined cochlear coordinate system to define the location of the modiolus, round window, and individual electrode contacts in the cochlear view to determine the AID for each electrode contact. The subsequent AID was used to approximate the cochlear place frequency based on the average SG map (Stakhovskaya et al. 2007), which is calculated by estimating the proportional distance from the base for the SG map, converting to the corresponding proportional distance along the organ of Corti (OC) map, and using Greenwoods equation to determine the associated frequency in Hz (Greenwood 1990). In the present study, landmarks were all determined by the first author. Complete insertion was defined as having all 12 electrode contacts located within the cochlea. It follows that partial insertion was defined as having at least one extracochlear electrode contact.

The cochlear duct length was measured on postoperative CT with OTOPLAN® using the elliptic-circular approximation (ECA) method, which has been demonstrated to be more accurate than previously described methodologies (Schurzig et al. 2018). This method determines the basal turn length of the lateral wall based on user-identified measurements of the cochlear diameter (*A*-value) and width (*B*-value), which are then used in the derivation of cochlear duct length.

Default Frequency Allocations

The default frequency filters for CI-alone and EAS device users were obtained using the manufacturer clinical software. For CI-alone users, the frequency range was 70-8500 Hz, which is logarithmically distributed across the active electrodes. For complete insertions, the subsequent default center frequencies for the 12 electrode contacts from apical to basal were as follows: 120, 235, 384, 579, 836, 1175, 1624, 2222, 3019, 4084, 5507, and 7410 Hz. For EAS device users, the clinical software assigns the low-frequency cutoff as the frequency at which unaided hearing thresholds exceed 65 dB HL, and logarithmically distributes the remaining mid-to-high frequency information across active electrodes. For both CI-alone and EAS devices, extracochlear electrode contacts were deactivated, and frequency filters were re-distributed across the remaining electrode contacts in accordance with clinical software recommendations.

Postoperative Speech Perception

The aided speech perception of CI-alone device users at 1, 3, and 6 months after CI activation was reviewed to assess the influence of a frequency-to-place mismatch on initial speech perception. Testing was completed in a soundproof booth with the participant seated 1 meter away from the sound source. Recorded materials were presented at 60 dB SPL. Speech perception was measured using the consonant-nucleus-consonant (CNC) word test (Peterson & Lehiste 1962), which is scored as the percent of words correctly repeated from a 50-word list. These scores were transformed into rationalized arcsine units (RAUs; Studebaker 1985) to normalize error variance. Word scores at 1, 3, and 6 months after CI activation were compared to the absolute value of the frequency-to-place mismatch. Absolute mismatch was evaluated based on the rationale that the detrimental effects on performance are likely to be comparable for positive and negative spectral mismatches, although there are no data confirming this. To minimize potential confounding variables, this analysis was restricted to CI-alone users who listened consistently to the default frequency filters, had a negative history of revision surgery or partial electrode array insertion, and completed testing at the aforementioned time intervals.

Quantifying Frequency-to-Place Mismatch

To quantify the extent of frequency-to-place mismatch, a fourth-order polynomial function was fit to the semitone deviation from the SG map as a function of AID for each ear. Absolute semitone deviation was quantified at 1500 Hz (approximately 267° on the SG map), which has been shown to be an important region for frequency alignment in vocoder simulation work (Baskent & Shannon 2007), and corresponds to the approximate spectral center of speech information required for recognition (ANSI/ASA 1997). Additionally, mismatch was quantified with regard to individual electrode contacts.

Quantifying Angular Separation Between Electrode Contacts

Angular separation between neighboring electrode contacts was measured for contacts residing within the 1-2 kHz region (approximately 224° to 333° on the average SG map) in CI-alone users. Again, this region was selected since it has been previously shown to contain important frequency information for speech recognition (ANSI/ASA 1997). Most participants had 2 electrode contacts located within this region; however, for those with 3 electrode contacts, angular distance between each pair of neighboring contacts was averaged. A smaller angular separation between neighboring contacts would be associated reduced peripheral selectivity and greater peripheral masking between channels.

Statistical Analysis

The D'Agostino-Pearson omnibus test was used to evaluate normality for continuous variables. For normally distributed data, a one-way analysis of variance (ANOVA) followed by a Tukey test for honestly significant differences (HSD) was performed. Pearson correlation was used to evaluate the relationship between AID of the most apical electrode contact and cochlear duct length. Multiple linear regression analysis was performed to model the relationship between AID of the most apical electrode contact and other factors (e.g., electrode array and AID of the most basal contact). Multiple linear regression was also used to assess the relationship between speech perception, degree of mismatch, and angular separation between electrode contacts. Statistical significance was defined as $p < 0.05$. Analyses were performed with SPSS version 25 for Windows (IBM Corp, Armonk, New York).

Results

Angular Insertion Depth and Cochlear Duct Length

The postoperative CTs of 111 ears (101 CI recipients) were reviewed. The mean age at implantation for all CI recipients was 64 ± 15.2 years. With respect to surgical approach, 106 (95.5%) electrode arrays were inserted through the round window and 5 (4.5%) were inserted through a cochleostomy. The majority of cases ($n = 106$, 95.5%) presented with a complete insertion of either the Flex24 ($n = 11$), Flex28 ($n = 48$), or FlexSOFT/Standard ($n = 47$) array. Figure 1 plots AID by array for complete insertions. The AID of the most apical electrode contact ranged from 389° to 751°, with a mean ± standard deviation of 579° ± 82.8°; electrode-specific values were 428° ± 34.3° for Flex24, 558° ± 65.4° for Flex28, and 636° ± 42.9° for FlexSOFT/Standard arrays. A one-way ANOVA demonstrated a statistically significant difference in AID across the three array types ($p < 0.001$). A post hoc Tukey HSD analysis revealed significant differences in apical AID for all three pairwise comparisons between arrays ($p < 0.001$). The AID of the most basal electrode contact was 7.1° ± 6.5° for Flex24 (range: 0° to 22°), 20.6° ± 13.1° for Flex28 (range: 0° to 62°), and 11.8° ± 10.4° for FlexSOFT/Standard (range: 0° to 54°) arrays, which were statistically different on ANOVA analysis ($p = 0.03$). A post hoc Tukey HSD analysis revealed significant differences in basal AID between Flex24 and Flex28 ($p = 0.003$) and Flex28 and FlexSOFT/Standard arrays ($p = 0.001$), and no difference between Flex24 and FlexSOFT/Standard ($p = 0.48$)[1].

The mean cochlear duct length was 34.0 mm ± 1.86 mm (range: 29.4 mm to 39.5 mm) for all participants. Figure 2 demonstrates the correlation between AID and cochlear duct length for complete insertions ($p < 0.05$ for all array types, individual r^2 values displayed in Fig. 2). A multiple linear regression model including cochlear duct length, AID of the most basal contact, and array type accounted for 84% of variance in AID of the most apical contact ($r^2 = 0.840$, $p < 0.001$). Coefficients appear in Table 1. Electrode type had a strong effect on apical AID; compared to the Flex24, apical AID rose by 114° with the Flex28 and 224° with the FlexSOFT/Standard. There was an increase of 19° in apical AID for every 1 mm reduction in cochlear duct length, and there was a 3° increase in apical AID for every 1° increment in basal AID.

Frequency-to-Place Mismatch: CI-Alone Users

Figure 3A plots the mean AID of the 12 electrode contacts for each array as a function of the default frequency filters for CI-alone device users with complete insertions; the SG cochlear place frequency is represented by the solid black line. The variability within each array type is additionally depicted in Figure 3B–D. Partial insertions are indicated with dotted lines. The mean deviation in semitones between the default electric center frequency and the predicted SG place frequency as a function of AID is demonstrated in Figure 4A. On average, the default frequency filters for Flex28 and FlexSOFT/Standard arrays fell approximately half an octave (one octave is equal to 12 semitones) below the predicted SG frequency for AIDs between 0° and 270°. In this same region, the default frequency filters for Flex24 arrays fell approximately an octave below the predicted SG frequency on average. Beyond 270°, differences from the tonotopic cochlear place across the arrays became more pronounced. FlexSOFT/Standard arrays maintained a relatively consistent mean frequency-to-place mismatch of approximately half an octave across the entire array, whereas the shorter arrays deviated by 1-2 octaves on average within the second turn of the cochlea (between 360° and 720°). These array-specific trends notwithstanding, there was substantial interindividual variability in frequency-to-place mismatch between participants implanted with the same array type, with partial insertion recipients generally showing greater mismatch (Fig. 4B–D).

[1]Shallower basal AID observed in the FlexSOFT/Standard cohort compared to the Flex28 cohort could reflect insertion resistance associated with increased array diameter near the stopper or the decrease in cross-sectional diameter of the scala tympani apically (Avci et al. 2014). The relatively shallow basal AID of Flex24 electrodes is likely due to a shorter distance between the stopper and basal-most contact compared to both Flex28 and FlexSOFT/Standard electrode arrays.

Frequency-to-Place Mismatch: EAS Users

Figure 5A plots the AID of each electrode contact as a function of the default electric frequency filters for individual EAS device users with complete insertions; results separated by array types appear in Figure 5B–D (following the same plotting conventions as Fig. 3). The deviation in semitones from the predicted SG frequency for EAS devices is shown in Figure 6. These data indicated a high degree of variability in frequency-to-place mismatch. Some EAS users demonstrated a close alignment between the default filters and the predicted SG frequencies, such that the low-frequency cutoff aligned with the place frequency associated with the apical electrode contact, but marked mismatches were observed for other EAS users. Data for the EAS devices can be generally categorized as follows: 1) insertion depths that extended into the cochlear region with functional acoustic hearing (positive semitone deviation of the most apical contact), 2) insertion depths that met the cochlear region with functional acoustic hearing (approx. zero semitone deviation of the most apical contact), and 3) insertion depths that did not reach the cochlear region with functional acoustic hearing (negative semitone deviation of the most apical contact). Negative deviations were more common than positive deviations or matches; the mean absolute deviation for the apical electrode in EAS users with a complete insertion was 8.78 semitones, and 38.5% of ears had an absolute deviation of ≤ 6 semitones (37% including one case with partial insertion).

Partial Insertion Cases

Partial insertions were rare and observed for only four CI-alone users and one EAS user, with each case having one extracochlear contact. The prevalence of extracochlear contacts by electrode array was: Flex24 (1/12, 8.3%), Flex28 (2/50, 4%), and FlexSOFT/Standard (2/49, 4.1%). Cases of partial insertions are denoted with dotted lines in Figures 3–6.

Quantifying Frequency-to-Place Mismatch

Figure 7 plots the absolute frequency-to-place mismatch in semitone deviation from the SG map at 1500 Hz for each array type in CI-alone users with complete insertions. Among these users, a one-way ANOVA demonstrated a statistically significant difference in absolute semitone deviation across the three array types ($p < 0.001$). A post hoc Tukey HSD analysis revealed significant differences between Flex24 and FlexSOFT/Standard ($p < 0.001$), and between Flex24 and Flex28 arrays ($p = 0.004$), with no significant difference noted when comparing Flex28 to FlexSOFT/Standard arrays ($p = 0.189$). When examining individuals implanted with the same array, the degree of mismatch varied as much as one octave with default frequency filters.

Postoperative Speech Perception

Given the significant variability observed in the AID of the apical electrode contact (Fig. 1) and frequency-to-place mismatch at 1500 Hz (Fig. 7) across and within arrays, we examined the relationship between these factors and postoperative speech perception for CI-alone users ($n = 48$). The top row of Figure 8 displays CNC word scores as a function of absolute frequency-to-place mismatch at 1500 Hz. Smaller degrees of frequency-to-place mismatch predicted better CNC word scores at the 1-month ($r = -0.367$, $p = 0.010$), 3-month ($r = -0.334$, $p = 0.021$), and 6-month ($r = -0.401$, $p = 0.005$) intervals. Partial correlations, controlling for age, resulted in the same pattern of significance. While the frequency-to-place mismatch was < 7 semitones for most subjects, it exceeded 9 semitones in five cases. When these 5 cases were removed from the model, mismatch was no longer significantly associated with CNC word scores. This raises the possibility that a criterion mismatch (e.g., > 7 semitones) may be necessary in order to observe a detrimental effect on speech perception.

The bottom row of Figure 8 demonstrates that the angular separation between electrode contacts located in the 1-2 kHz region on the SG map was positively correlated with CNC word scores at the 1-month ($r = 0.361$, $p = 0.012$) and 6-month ($r = 0.446$, $p = 0.002$) intervals, and trended towards significance at the 3-month interval ($r = 0.263$, $p = 0.072$). Interestingly, frequency-to-place mismatch and angular separation between electrodes were not correlated ($p = 0.628$). A regression model demonstrated that both reduced frequency-to-place mismatch ($p < 0.001$) and greater angular separation between electrode contacts ($p < 0.001$) were associated with better CNC word scores, with coefficients appearing in Table 2. This model also demonstrates an improvement in word scores across intervals ($p < 0.001$). Thus, frequency-to-place mismatch and peripheral masking appear to contribute independently to speech perception.

The degree of mismatch in semitones between the center frequency associated with each electrode contact and the corresponding SG place frequency was also quantified. Table 3 shows default center frequencies for each channel and mean AID with the corresponding predicted SG frequency for each electrode contact by array. Individual values for each participant can be found in Appendix A. Table 4 reports correlations between the magnitude of the frequency-to-place mismatch in semitones and CNC word scores in RAUs at 6 months for the CI-alone cohort. These correlations were significant and negative for electrodes 1 through 6; correlations failed to reach significance for electrodes 7 through 12, which generally correspond to the tonotopic regions > 2000 Hz on the SG map (Table 3).

Discussion

CI-alone and EAS device users experience variability in frequency-to-place mismatch, which may contribute to variability in speech perception previously reported for these cohorts (Gantz et al. 1993; Blamey et al. 1996; Green et al. 2007; Polak et al. 2010; Lazard et al. 2012; Blamey et al. 2013; Dillon et al. 2014; Gifford et al. 2017). The magnitude of this mismatch depends upon the array length, frequency filters, and interindividual differences in cochlear size. Additional factors contribute in the case of EAS users, as default mapping procedures also incorporate unaided hearing thresholds (which cannot be determined until *after* the array of pre-determined length has been inserted) into the assignment of electric frequency filters. The primary aim of the present study was to characterize the extent of frequency-to-place mismatch in a large cohort of CI-alone and EAS device users with lateral wall arrays. As expected, our results indicated that the frequency-to-place mismatch is minimized by a deep insertion for CI-alone device users when using the default frequency filters of 70-8500 Hz. Results are consistent with substantial differences in the extent of mismatch between recipients implanted with the same array and provide additional evidence that smaller degrees of mismatch may serve as a potential mechanism for improved speech perception in the CI-alone condition. Furthermore, this is the first study to our knowledge to quantify the significant variability of frequency-to-place mismatch that exists within EAS device users.

Variability in Frequency-to-Place Mismatch Among CI-Alone and EAS Users

Previous work by Landsberger et al. (2015) examined the relationship between insertion depth and CI-alone default frequency filters in a cohort of Flex28 ($n = 5$) and Standard ($n = 13$) arrays using x-ray to estimate electrode position in the cochlea. The observed insertion angles in that study are similar to previous estimates (Hamzavi & Arnoldner 2006; Radeloff et al. 2008), yet somewhat smaller compared to data from other studies (Boyd 2011; Franke-Trieger et al. 2014; O'Connell et al. 2017; Canfarotta et al. 2019) and the present study. Specifically, we observed average insertion angles of 558° for 28 mm arrays and 636° for 31.5 mm arrays, whereas Landsberger et al. (2015) reported insertion angles of 471° and 544°, respectively. Similar to Vermeire et al. (2015), we observed a half-octave deviation from the SG frequency within the basal turn of the cochlea as opposed to the full octave previously reported (Landsberger et al. 2015); these differences may be due to greater depths of insertion and differences in default frequency filters (100-8500 Hz in Landsberger et al. (2015)). Our results corroborate findings that the variation in frequency deviation from the SG map becomes most evident beyond 270° (Landsberger et al. 2015), where consistent differences between Flex28 and FlexSOFT/Standard arrays emerge. While the mean frequency-to-place mismatch for specific electrode arrays provides valuable insight, perhaps the more striking finding is the wide range of individual differences in the extent of mismatch amongst CI-alone users who underwent complete insertion of the same array.

One key consideration is that the magnitude of the frequency-to-place mismatch is dependent on the electric frequency filters. Participants in the present study were mapped using the FS4 coding strategy, with filter settings of 70-8500 Hz. In contrast, the HDCIS coding strategy uses default filter settings of 250-8500 Hz; if our participants had received a default HDCIS map, then the mismatch would have been smaller for the Flex28 arrays than the FlexSOFT/Standard and Flex24 arrays. In a study of 5 MED-EL Combi40+ array recipients with insertion depths greater than 600°, Gani et al. (2007) demonstrated an improvement in speech perception with deactivation of apical electrodes. Participants in that study had center frequencies > 250 Hz for the most apical contact, suggesting that deactivation of apical electrodes resulted in a closer tonotopic alignment and conferred speech perception benefit. An alternative explanation for the noted improvements in performance could be that deactivation of apical electrodes reduced channel interaction in this region (Arnoldner et al. 2007; Kalkman et al. 2014; Landsberger et al. 2014).

To our knowledge, this is the first study to quantify the degree of mismatch that results from default electric frequency filters in EAS devices, which are determined in part by the aidable low-frequency range for each patient. Shorter lateral wall arrays with a shallow AID confer a greater likelihood of hearing preservation (Gantz et al. 2016; Suhling et al. 2016; O'Connell et al. 2017). However, Flex24 array recipients in the CI-alone condition display a greater degree of mismatch than those implanted with longer arrays when current mapping procedures are followed. With improvements in surgical technique and electrode array design, several groups have investigated hearing preservation rates with longer flexible lateral wall arrays (Tamir et al. 2012; Mick et al. 2014; Usami et al. 2014; Moteki et al. 2018), which would provide greater cochlear coverage and less mismatch if residual hearing were to be lost. While hearing preservation was not a focus of the present study, we have demonstrated that there are a number of EAS device users with 28 and 31.5 mm arrays. These longer arrays are more likely to reach the region that is aided acoustically, resulting in overlapping acoustic and electric stimulation. This consideration may be relevant in mapping EAS devices, as ipsilateral electric and acoustic stimulation can mask one another (Kruger et al. 2017; Imsiecke et al. 2018). To date, it remains difficult to predict the postoperative unaided hearing thresholds, which influence the electric frequency filters for EAS devices. Therefore, selecting the electrode array length preoperatively that minimizes the distance between the location of the most apical contact and the highest aidable acoustic frequency is challenging in hearing preservation cases. This challenge is reflected in the fact that only 37% of EAS users had a mismatch of ≤ 6 semitones on the most apical contact. The resultant frequency-to-place mismatch may be mitigated by place-based mapping procedures using postoperative imaging algorithms to align the electric frequency filters with the cochlear place frequency (Dillon, O’Connell, et al., 2019).

It should be noted that partial insertions result in shallower insertion angles, thus contributing to frequency-to-place mismatch. Partial insertions may be intentional (e.g., in hearing preservation cases, anatomic variations, or resistance) or related to extrusion after placement. At our institution, complete insertion is the goal in all cases; however, partial insertions may be preferable if resistance is encountered during insertion. Previous work has demonstrated partial insertion rates as high as 32% with longer lateral wall arrays (De Seta et al. 2016; Holder et al. 2018). In contrast, the overall rate of partial insertion observed herein was 5%. The ability to achieve complete insertions in the majority of cases with longer arrays is an important finding for CI-alone users with default frequency filters, as deeper insertions result in improved speech perception (Buchman et al. 2014; O’Connell et al. 2016). Additionally, early identification of a partial insertion is crucial, so that extracochlear contacts can be deactivated at initial activation to avoid re-acclimatization to shifted electric frequency filters later.

Relationship Between Frequency-to-Place Mismatch and CI-Alone Speech Perception

While the present dataset demonstrates substantial variability in frequency-to-place mismatch among lateral wall array recipients, the clinical significance of this mismatch remains unclear. The human auditory system displays a remarkable degree of plasticity in adapting to tonotopically mismatched frequency information in CI recipients over time (Svirsky et al. 2004; Reiss et al. 2007; Reiss et al. 2014). Although CI users can learn to use frequency-shifted information, there is evidence that this adaptation can prolong the acclimatization period and, in some instances, may remain incomplete even after extensive listening experience (Svirsky et al. 2004; Sagi et al. 2010; Reiss et al. 2014; Svirsky et al. 2015; Tan et al. 2017). While Reiss et al. (2007) demonstrated that CI recipients are capable of adapting to shifts as large as 3 octaves, results of the present study suggest that smaller mismatches may limit performance for some CI-alone users at 6 months.

Similar to the present study, Venail et al. (2015) examined the relationship between frequency-to-place mismatch and speech perception in 24, 28, and 31.5 mm lateral wall array recipients. In contrast to the present findings, their results demonstrated that mismatch can be minimized with insertion of a 28 mm array (mean AID: 478°), which resulted in the shortest time to achieve maximum speech perception score, whereas 24 and 31.5 mm insertions resulted in greater mismatch in either direction, leading to longer acclimatization times. One methodological difference that could account for the discrepancies in conclusions of that study and the present one is related to the frequency-to-place function used to determine mismatch. As described by Stakhovskaya et al. (2007), the present study estimated SG place frequencies by: 1) using AID to estimate proportional distance from the base for the SG map, 2) determining the corresponding proportional distance along the OC map, and 3) using percentage from the apex in the OC to estimate frequency based on Greenwood's equation (Greenwood 1990). In contrast, it appears that the estimates of Venail et al. (2015) did not incorporate the transformation from SG to OC maps. Another difference is that Venail et al. (2015) determined position along the lateral wall, as described by Escude et al. (2006), rather than position relative to the OC (Alexiades et al. 2015). These methodological differences resulted in lower SG place frequencies for given insertion angles than previously described by Stakhovskaya et al. (2007) and reported in the present study.

Other groups have examined the relationship between AID, which can be thought of as a marker for frequency-to-place mismatch, and speech perception in the CI-alone condition. While Holden et al. (2013) demonstrated a negative correlation between depth of insertion and speech perception, the majority of participants included were implanted with a pre-curved array. Emerging evidence supports the notion that the impact of AID on speech perception depends on electrode array design. While greater depth of insertion improves outcomes with lateral wall arrays in the CI-alone condition (O'Connell et al. 2017), a shallower insertion with a pre-curved array optimizes modiolar proximity and confers benefit (Chakravorti et al. 2019). The benefits conferred by modiolar proximity must be weighed against the higher translocation rates of pre-curved arrays into the scala vestibuli (Wanna et al. 2014; Boyer et al. 2015), which has been shown to negatively impact speech perception (O'Connell et al. 2016; Chakravorti et al. 2019). These studies support the notion that when restricting the analysis to lateral wall arrays, deeper insertions are associated with improved speech perception. The results herein suggest that this benefit is in part related to closer tonotopic alignment with default frequency filters, which may have varying degrees of importance across cochlear regions.

Previous vocoder simulation work by Baskent and Shannon (2007) investigated the effect of spectral mismatch on speech perception and demonstrated better performance with a frequency matched map, particularly with alignment in the 1 to 2 kHz region, which has been shown to contain important information for speech intelligibility (ANSI/ASA 1997). Within our cohort, we observed the strongest correlation between frequency-to-place mismatch and early speech perception on electrode 5 (Table 4), which is generally located within the tonotopic region corresponding between 1 to 2 kHz (Table 3). When using default frequency filters, deeper insertion of a lateral wall array tends to minimize the frequency-to-place mismatch within this region. Additionally, as recent work has focused on the role of place-based mapping procedures which account for tonotopicity (Grasmeder et al. 2014;

Jiam et al. 2016; Jiam et al. 2018; Dillon, O'Connell, et al. 2019), our findings highlight that it may be advantageous to align electric frequency information from the apex at least through the 2 kHz region, which corresponds to the basal turn of the cochlea. It is possible that aligning information at higher frequencies may also be of importance, but smaller interindividual variability in this region precluded the present study from demonstrating benefit.

Frequency-to-Place Mismatch versus Peripheral Masking

While reduction in frequency-to-place mismatch offers one possible mechanism for the speech perception benefit gained with deeply inserted lateral wall arrays, it can be challenging to differentiate these effects from the simultaneous advantage of reduced peripheral masking with greater angular separation between electrode contacts on longer arrays. To a certain extent, these mechanisms are intrinsically related. In Figure 9, we illustrate four different scenarios in an attempt to disambiguate these two factors. Panel A displays a deeply inserted 31.5 mm array in an individual with a short cochlear duct length, which results in a small degree of frequency-to-place mismatch (E6 and E7 shown in green, mismatch < 2 semitones) and large angular separation between electrode contacts. Theoretically, in addition to the benefit associated with little or no frequency-to-place mismatch, this supports more selective stimulation of discrete neuronal populations along the SG. Panel B demonstrates that when this same array is implanted in an individual with a longer cochlear duct, the same linear insertion depth will result in a shallower AID (E5 and E6 depicted with red stripes, mismatch ~ 6 semitones). This case is characterized by relatively smaller angular separation between contacts and crowding of spectral information. Panel C further illustrates that if individual B had a deeper basal insertion depth, mismatch would be reduced, yet there would be no change in angular separation between contacts. Finally, Panel D shows that further complexity is introduced with different electrode array lengths and closer proximity of neighboring electrode contacts with shorter arrays.

Based on the examples illustrated in Figure 9, it is not entirely surprising that a reduction in mismatch and greater angular separation between electrode contacts were both correlated with CNC word scores in the present study. This finding supports the use of a longer (31.5 mm) array in patients destined for the CI-alone condition to gain benefit from both closer tonotopic alignment when using default frequency filters and greater separation between electrode contacts. However, it is essential to note that a complete insertion may not always be feasible in an individual with a small cochlea (e.g., < 30 mm cochlear duct length). With recent work focusing on precision cochlear implantation, preoperative measurement of cochlear duct length may assist in the electrode array selection process and identify such cases in which a 28 mm array may be more appropriate.

Limitations and Future Work

It is generally accepted that CIs stimulate SG cells; as such, the average SG map is frequently cited in relevant CI literature and was used herein to estimate frequency-to-place maps (Stakhovskaya et al. 2007). That being said, the exact electric frequency-to-place map for CI users remains unclear (Dorman et al. 2007). In patients with residual low-frequency hearing, it is possible that distal SG dendrites or surviving hair cells at the level of the

OC influence the apical frequency-to-place map. Some have suggested averaging SG and OC place frequencies, assuming that the electrode array is positioned between the two structures (Rader et al. 2016). Recently, Li et al. (2019) used synchrotron-radiation phase-contrast imaging with three-dimensional reconstructions to analyze SG anatomy and its relationship to the OC. The average length of reproduced spiral ganglions was similar to that reported by Stakhovskaya et al. (2007). While the average SG map was used to estimate frequency-to-place mismatch in the present study, individual variability in the relationship between AID and characteristic frequency introduces the possibility that SG maps could be individualized for each CI recipient. However, as individual maps are inherently dependent upon an accurate calculation of cochlear duct length, we are limited with current *in vivo* estimation errors of ~5% largely due to the inability to account for variability in cochlear morphology beyond the second turn (Koch et al. 2017). In the future, technological advances will likely allow for a personalized approach with clinical imaging modalities. Additionally, future work is needed to determine whether an SG (Stakhovskaya et al. 2007) or OC map (Greenwood 1990) is closer to the perceived frequency in CI recipients.

Although there is an association between frequency-to-place mismatch and CNC word scores at the group level, this effect appears to be driven by a small number of subjects with frequency-to-place > 7 semitones. If this finding is replicated in future research, it could reflect error in estimating frequency-to-place mismatch, or individual differences across CI users. It is also possible that a certain degree of mismatch can be tolerated before a detrimental effect to speech perception is observed.

As frequency-to-place mismatch plays a role in early speech perception amongst CI-alone users, it seems reasonable to speculate that a similar benefit might be observed among EAS device users. However, as a higher low-frequency cutoff generally supports a closer tonotopic alignment, it is difficult to disentangle effects related to low-frequency residual acoustic hearing, frequency-to-place mismatch, and peripheral masking. Manipulation of electric frequency filters in individual patients could disambiguate these factors. Prospective studies evaluating place-based versus default mapping procedures are currently underway.

Conclusions

The present report demonstrated the wide variability in frequency-to-place mismatch in a large cohort of lateral wall array recipients listening with CI-alone and EAS devices. On average, deep lateral wall insertions with default frequency filters minimized frequency-to-place mismatch, which may account for the speech perception benefit observed in CI-alone device users implanted with longer arrays. There was wide variation in frequency-to-place mismatch for both CI-alone and EAS device users, dependent upon the AID of the array and, in the case of EAS, the edge frequency associated with residual hearing. For CI users with no aidable residual hearing, smaller frequency-to-place mismatches at 1500 Hz were associated with better CNC word scores, independent of effects related to reductions in peripheral masking associated with greater contact spacing on longer arrays. This observation has provided additional evidence to support the possibility that incorporating array AID into individualized electric frequency filters, as used in a place-based mapping procedure, may improve performance.

Supplementary Material

Refer to Web version on PubMed Central for supplementary material.

Financial Disclosures/Conflicts of Interest:

This project was funded in part by the NIH through NIDCD (T32 DC005360). HCP, KDB, and BPO have served on the surgical advisory board for MED-EL Corporation. HCP is a consultant for MED-EL Corporation. BPO is a consultant for Advanced Bionics and Johnson and Johnson. MTD is supported by a research grant from MED-EL Corporation provided to the university. MWC and EB declare that involvement in research was conducted in the absence of any commercial or financial relationships that could be construed as a potential conflict of interest.

This project was funded in part by the NIH through NIDCD (T32 DC005360). HCP, KDB, and BPO have served on the surgical advisory board for MED-EL Corporation. HCP is a consultant for MED-EL Corporation. BPO is a consultant for Advanced Bionics and Johnson and Johnson. MTD is supported by a research grant from MED-EL Corporation provided to the university. MWC and EB declare that involvement in research was conducted in the absence of any commercial or financial relationships that could be construed as a potential conflict of interest.

References

Alexiades G, Dhanasingh A, Jolly C (2015). Method to estimate the complete and two-turn cochlear duct length. Otol Neurotol, 36, 904–907. [PubMed: 25299827]

ANSI/ASA. (1997). American National Standard Methods for Calculation of the Speech Intelligibility Index. American National Standards Institute, New York, S3.5.

Arnoldner C, Riss D, Baumgartner WD, et al. (2007). Cochlear implant channel separation and its influence on speech perception--implications for a new electrode design. Audiol Neurootol, 12, 313–324. [PubMed: 17536200]

Avci E, Nauwelaers T, Lenarz T, et al. (2014). Variations in microanatomy of the human cochlea. J Comp Neurol, 522, 3245–3261. [PubMed: 24668424]

Baskent D, Shannon RV (2007). Combined effects of frequency compression-expansion and shift on speech recognition. Ear Hear, 28, 277–289. [PubMed: 17485977]

Blamey P, Arndt P, Bergeron F, et al. (1996). Factors affecting auditory performance of postlinguistically deaf adults using cochlear implants. Audiol Neurootol, 1, 293–306. [PubMed: 9390810]

Blamey P, Artieres F, Baskent D, et al. (2013). Factors affecting auditory performance of postlinguistically deaf adults using cochlear implants: an update with 2251 patients. Audiol Neurootol, 18, 36–47. [PubMed: 23095305]

Boyd PJ (2011). Potential benefits from deeply inserted cochlear implant electrodes. Ear Hear, 32, 411–427. [PubMed: 21248642]

Boyer E, Karkas A, Attye A, et al. (2015). Scalar localization by cone-beam computed tomography of cochlear implant carriers: a comparative study between straight and periomodiolar precurved electrode arrays. Otol Neurotol, 36, 422–429. [PubMed: 25575374]

Buchman CA, Dillon MT, King ER, et al. (2014). Influence of cochlear implant insertion depth on performance: a prospective randomized trial. Otol Neurotol, 35, 1773–1779. [PubMed: 25122601]

Buchner A, Illg A, Majdani O, et al. (2017). Investigation of the effect of cochlear implant electrode length on speech comprehension in quiet and noise compared with the results with users of electro-acoustic-stimulation, a retrospective analysis. PLoS One, 12, e0174900. [PubMed: 28505158]

Canfarotta MW, Dillon MT, Buss E, et al. (2019). Validating a New Tablet-based Tool in the Determination of Cochlear Implant Angular Insertion Depth. Otol Neurotol, 40, 1006–1010. [PubMed: 31290802]

Chakravorti S, Noble JH, Gifford RH, et al. (2019). Further Evidence of the Relationship Between Cochlear Implant Electrode Positioning and Hearing Outcomes. Otol Neurotol.

De Seta D, Nguyen Y, Bonnard D, et al. (2016). The Role of Electrode Placement in Bilateral Simultaneously Cochlear-Implanted Adult Patients. Otolaryngol Head Neck Surg, 155, 485–493. [PubMed: 27165685]

Dhanasingh A, Jolly C (2017). An overview of cochlear implant electrode array designs. Hear Res, 356, 93–103. [PubMed: 29102129]

Dillon MT, Buss E, Adunka OF, et al. (2015). Influence of Test Condition on Speech Perception With Electric-Acoustic Stimulation. Am J Audiol, 24, 520–528. [PubMed: 26650652]

Dillon MT, Buss E, Pillsbury HC, et al. (2014). Effects of hearing aid settings for electric-acoustic stimulation. J Am Acad Audiol, 25, 133–140. [PubMed: 24828214]

Dillon MT, Buss E, Rooth MA, et al. (2019). Low-frequency pitch perception in cochlear implant recipients with normal hearing in the contralateral ear. J Speech Lang Hear Res.

Dillon MT, O'Connell BP, Canfarotta MW, et al. (2019). Incorporating electrode angular insertion depth in electric-acoustic stimulation programming. Podium Presentation at the 46th Annual Scientific and Technology Meeting of the American Auditory Society, Scottsdale, AZ.

Dorman MF, Spahr T, Gifford R, et al. (2007). An electric frequency-to-place map for a cochlear implant patient with hearing in the nonimplanted ear. J Assoc Res Otolaryngol, 8, 234–240. [PubMed: 17351713]

Dunn CC, Perreau A, Gantz B, et al. (2010). Benefits of localization and speech perception with multiple noise sources in listeners with a short-electrode cochlear implant. J Am Acad Audiol, 21, 44–51. [PubMed: 20085199]

Escude B, James C, Deguine O, et al. (2006). The size of the cochlea and predictions of insertion depth angles for cochlear implant electrodes. Audiol Neurootol, 11 Suppl 1, 27–33. [PubMed: 17063008]

Finley CC, Holden TA, Holden LK, et al. (2008). Role of electrode placement as a contributor to variability in cochlear implant outcomes. Otol Neurotol, 29, 920–928. [PubMed: 18667935]

Franke-Trieger A, Jolly C, Darbinjan A, et al. (2014). Insertion depth angles of cochlear implant arrays with varying length: a temporal bone study. Otol Neurotol, 35, 58–63. [PubMed: 24335932]

Gani M, Valentini G, Sigrist A, et al. (2007). Implications of deep electrode insertion on cochlear implant fitting. J Assoc Res Otolaryngol, 8, 69–83. [PubMed: 17216585]

Gantz BJ, Dunn C, Oleson J, et al. (2016). Multicenter clinical trial of the Nucleus Hybrid S8 cochlear implant: Final outcomes. Laryngoscope, 126, 962–973. [PubMed: 26756395]

Gantz BJ, Hansen MR, Turner CW, et al. (2009). Hybrid 10 clinical trial: preliminary results. Audiol Neurootol, 14 Suppl 1, 32–38. [PubMed: 19390173]

Gantz BJ, Woodworth GG, Knutson JF, et al. (1993). Multivariate predictors of audiological success with multichannel cochlear implants. Ann Otol Rhinol Laryngol, 102, 909–916. [PubMed: 8285510]

Gifford RH, Davis TJ, Sunderhaus LW, et al. (2017). Combined Electric and Acoustic Stimulation With Hearing Preservation: Effect of Cochlear Implant Low-Frequency Cutoff on Speech Understanding and Perceived Listening Difficulty. Ear Hear, 38, 539–553. [PubMed: 28301392]

Gifford RH, Dorman MF (2012). The Psychophysics of Low-Frequency Acoustic Hearing in Electric and Acoustic Stimulation (Eas) and Bimodal Patients. J Hear Sci, 2, 33–44. [PubMed: 24244874]

Gifford RH, Dorman MF, Sheffield SW, et al. (2014). Availability of binaural cues for bilateral implant recipients and bimodal listeners with and without preserved hearing in the implanted ear. Audiol Neurootol, 19, 57–71. [PubMed: 24356514]

Gifford RH, Dorman MF, Skarzynski H, et al. (2013). Cochlear implantation with hearing preservation yields significant benefit for speech recognition in complex listening environments. Ear Hear, 34, 413–425. [PubMed: 23446225]

Grasmeder ML, Verschuur CA, Batty VB (2014). Optimizing frequency-to-electrode allocation for individual cochlear implant users. J Acoust Soc Am, 136, 3313. [PubMed: 25480076]

Green KM, Bhatt Y, Mawman DJ, et al. (2007). Predictors of audiological outcome following cochlear implantation in adults. Cochlear Implants Int, 8, 1–11. [PubMed: 17479968]

Greenwood DD (1990). A cochlear frequency-position function for several species--29 years later. J Acoust Soc Am, 87, 2592–2605. [PubMed: 2373794]

Hamzavi J, Arnoldner C (2006). Effect of deep insertion of the cochlear implant electrode array on pitch estimation and speech perception. Acta Otolaryngol, 126, 1182–1187. [PubMed: 17050311]

Hardy M (1938). The length of the organ of corti in man. Am J Anat., 63, 291–311.

Helbig S, Van de Heyning P, Kiefer J, et al. (2011). Combined electric acoustic stimulation with the PULSARCI(100) implant system using the FLEX(EAS) electrode array. Acta Otolaryngol, 131, 585–595. [PubMed: 21281057]

Hochmair I, Arnold W, Nopp P, et al. (2003). Deep electrode insertion in cochlear implants: apical morphology, electrodes and speech perception results. Acta Otolaryngol, 123, 612–617. [PubMed: 12875584]

Holden LK, Finley CC, Firszt JB, et al. (2013). Factors affecting open-set word recognition in adults with cochlear implants. Ear Hear, 34, 342–360. [PubMed: 23348845]

Holder JT, Kessler DM, Noble JH, et al. (2018). Prevalence of Extracochlear Electrodes: Computerized Tomography Scans, Cochlear Implant Maps, and Operative Reports. Otol Neurotol, 39, e325–e331. [PubMed: 29738386]

Imsiecke M, Kruger B, Buchner A, et al. (2018). Electric-acoustic forward masking in cochlear implant users with ipsilateral residual hearing. Hear Res, 364, 25–37. [PubMed: 29673567]

Jiam NT, Gilbert M, Cooke D, et al. (2018). Association Between Flat-Panel Computed Tomographic Imaging-Guided Place-Pitch Mapping and Speech and Pitch Perception in Cochlear Implant Users. JAMA Otolaryngol Head Neck Surg.

Jiam NT, Pearl MS, Carver C, et al. (2016). Flat-Panel CT Imaging for Individualized Pitch Mapping in Cochlear Implant Users. Otol Neurotol, 37, 672–679. [PubMed: 27273394]

Kalkman RK, Briaire JJ, Dekker DM, et al. (2014). Place pitch versus electrode location in a realistic computational model of the implanted human cochlea. Hear Res, 315, 10–24. [PubMed: 24975087]

Koch RW, Elfarnawany M, Zhu N, et al. (2017). Evaluation of Cochlear Duct Length Computations Using Synchrotron Radiation Phase-Contrast Imaging. Otol Neurotol, 38, e92–e99. [PubMed: 28595256]

Kruger B, Buchner A, Nogueira W (2017). Simultaneous masking between electric and acoustic stimulation in cochlear implant users with residual low-frequency hearing. Hear Res, 353, 185–196. [PubMed: 28688755]

Landsberger DM, Marozeau J, Mertens G, et al. (2018). The relationship between time and place coding with cochlear implants with long electrode arrays. J Acoust Soc Am, 144, EL509. [PubMed: 30599674]

Landsberger DM, Mertens G, Punte AK, et al. (2014). Perceptual changes in place of stimulation with long cochlear implant electrode arrays. J Acoust Soc Am, 135, EL75–81. [PubMed: 25234918]

Landsberger DM, Svrakic M, Roland JT Jr., et al. (2015). The Relationship Between Insertion Angles, Default Frequency Allocations, and Spiral Ganglion Place Pitch in Cochlear Implants. Ear Hear, 36, e207–213. [PubMed: 25860624]

Lazard DS, Vincent C, Venail F, et al. (2012). Pre-, per- and postoperative factors affecting performance of postlinguistically deaf adults using cochlear implants: a new conceptual model over time. PLoS One, 7, e48739. [PubMed: 23152797]

Li H, Schart-Moren N, Rohani SA, et al. (2019). Synchrotron Radiation-Based Reconstruction of the Human Spiral Ganglion: Implications for Cochlear Implantation. Ear Hear.

Meng J, Li S, Zhang F, et al. (2016). Cochlear Size and Shape Variability and Implications in Cochlear Implantation Surgery. Otol Neurotol, 37, 1307–1313. [PubMed: 27579839]

Mick P, Amoodi H, Shipp D, et al. (2014). Hearing preservation with full insertion of the FLEXsoft electrode. Otol Neurotol, 35, e40–44. [PubMed: 24080974]

Moteki H, Nishio SY, Miyagawa M, et al. (2018). Feasibility of hearing preservation for residual hearing with longer cochlear implant electrodes. Acta Otolaryngol, 138, 1080–1085. [PubMed: 30702034]

O'Connell BP, Cakir A, Hunter JB, et al. (2016). Electrode Location and Angular Insertion Depth Are Predictors of Audiologic Outcomes in Cochlear Implantation. Otol Neurotol, 37, 1016–1023. [PubMed: 27348391]

O'Connell BP, Hunter JB, Haynes DS, et al. (2017). Insertion depth impacts speech perception and hearing preservation for lateral wall electrodes. Laryngoscope, 127, 2352–2357. [PubMed: 28304096]

Peterson GE, Lehiste I (1962). Revised CNC lists for auditory tests. J Speech Hear Disord, 27, 62–70. [PubMed: 14485785]

Pillsbury HC 3rd, Dillon MT, Buchman CA, et al. (2018). Multicenter US Clinical Trial With an Electric-Acoustic Stimulation (EAS) System in Adults: Final Outcomes. Otol Neurotol, 39, 299–305. [PubMed: 29342054]

Polak M, Lorens A, Helbig S, et al. (2010). Fitting of the hearing system affects partial deafness cochlear implant performance. Cochlear Implants Int, 11 Suppl 1, 117–121.

Prentiss S, Staecker H, Wolford B (2014). Ipsilateral acoustic electric pitch matching: a case study of cochlear implantation in an up-sloping hearing loss with preserved hearing across multiple frequencies. Cochlear Implants Int, 15, 161–165. [PubMed: 24601768]

Radeloff A, Mack M, Baghi M, et al. (2008). Variance of angular insertion depths in free-fitting and perimodiolar cochlear implant electrodes. Otol Neurotol, 29, 131–136. [PubMed: 18090204]

Rader T, Doge J, Adel Y, et al. (2016). Place dependent stimulation rates improve pitch perception in cochlear implantees with single-sided deafness. Hear Res, 339, 94–103. [PubMed: 27374479]

Rader T, Fastl H, Baumann U (2013). Speech perception with combined electric-acoustic stimulation and bilateral cochlear implants in a multisource noise field. Ear Hear, 34, 324–332. [PubMed: 23263408]

Reiss LA, Turner CW, Erenberg SR, et al. (2007). Changes in pitch with a cochlear implant over time. J Assoc Res Otolaryngol, 8, 241–257. [PubMed: 17347777]

Reiss LA, Turner CW, Karsten SA, et al. (2014). Plasticity in human pitch perception induced by tonotopically mismatched electro-acoustic stimulation. Neuroscience, 256, 43–52. [PubMed: 24157931]

Sagi E, Fu QJ, Galvin JJ 3rd, et al. (2010). A model of incomplete adaptation to a severely shifted frequency-to-electrode mapping by cochlear implant users. J Assoc Res Otolaryngol, 11, 69–78. [PubMed: 19774412]

Schatzer R, Vermeire K, Visser D, et al. (2014). Electric-acoustic pitch comparisons in single-sided-deaf cochlear implant users: frequency-place functions and rate pitch. Hear Res, 309, 26–35. [PubMed: 24252455]

Schurzig D, Timm ME, Batsoulis C, et al. (2018). A Novel Method for Clincial Cochlear Duct Length Estimation toward Patient-Specific Cochlear Implant Selection. OTO Open, 1–8.

Stakhovskaya O, Sridhar D, Bonham BH, et al. (2007). Frequency map for the human cochlear spiral ganglion: implications for cochlear implants. J Assoc Res Otolaryngol, 8, 220–233. [PubMed: 17318276]

Studebaker GA (1985). A "rationalized" arcsine transform. J Speech Hear Res, 28, 455–462. [PubMed: 4046587]

Suhling MC, Majdani O, Salcher R, et al. (2016). The Impact of Electrode Array Length on Hearing Preservation in Cochlear Implantation. Otol Neurotol, 37, 1006–1015. [PubMed: 27309713]

Svirsky MA, Fitzgerald MB, Sagi E, et al. (2015). Bilateral cochlear implants with large asymmetries in electrode insertion depth: implications for the study of auditory plasticity. Acta Otolaryngol, 135, 354–363. [PubMed: 25719506]

Svirsky MA, Silveira A, Neuburger H, et al. (2004). Long-term auditory adaptation to a modified peripheral frequency map. Acta Otolaryngol, 124, 381–386. [PubMed: 15224858]

Tamir S, Ferrary E, Borel S, et al. (2012). Hearing preservation after cochlear implantation using deeply inserted flex atraumatic electrode arrays. Audiol Neurootol, 17, 331–337. [PubMed: 22813984]

Tan CT, Martin B, Svirsky MA (2017). Pitch Matching between Electrical Stimulation of a Cochlear Implant and Acoustic Stimuli Presented to a Contralateral Ear with Residual Hearing. J Am Acad Audiol, 28, 187–199. [PubMed: 28277210]

Usami S, Moteki H, Tsukada K, et al. (2014). Hearing preservation and clinical outcome of 32 consecutive electric acoustic stimulation (EAS) surgeries. Acta Otolaryngol, 134, 717–727. [PubMed: 24834939]

Venail F, Mathiolon C, Menjot de Champfleur S, et al. (2015). Effects of electrode array length on frequency-place mismatch and speech perception with cochlear implants. Audiol Neurootol, 20, 102–111. [PubMed: 25678235]

Vermeire K, Landsberger DM, Van de Heyning PH, et al. (2015). Frequency-place map for electrical stimulation in cochlear implants: Change over time. Hear Res, 326, 8–14. [PubMed: 25840373]

Wanna GB, Noble JH, Carlson ML, et al. (2014). Impact of electrode design and surgical approach on scalar location and cochlear implant outcomes. Laryngoscope, 124 Suppl 6, S1–7.

Wess JM, Brungart DS, Bernstein JGW (2017). The Effect of Interaural Mismatches on Contralateral Unmasking With Single-Sided Vocoders. Ear Hear, 38, 374–386. [PubMed: 28002083]

Won JH, Drennan WR, Rubinstein JT (2007). Spectral-ripple resolution correlates with speech reception in noise in cochlear implant users. J Assoc Res Otolaryngol, 8, 384–392. [PubMed: 17587137]

Wurfel W, Lanfermann H, Lenarz T, et al. (2014). Cochlear length determination using Cone Beam Computed Tomography in a clinical setting. Hear Res, 316, 65–72. [PubMed: 25124151]

Yukawa K, Cohen L, Blamey P, et al. (2004). Effects of insertion depth of cochlear implant electrodes upon speech perception. Audiol Neurootol, 9, 163–172. [PubMed: 15084821]

Zhou N (2017). Deactivating stimulation sites based on low-rate thresholds improves spectral ripple and speech reception thresholds in cochlear implant users. J Acoust Soc Am, 141, EL243. [PubMed: 28372106]

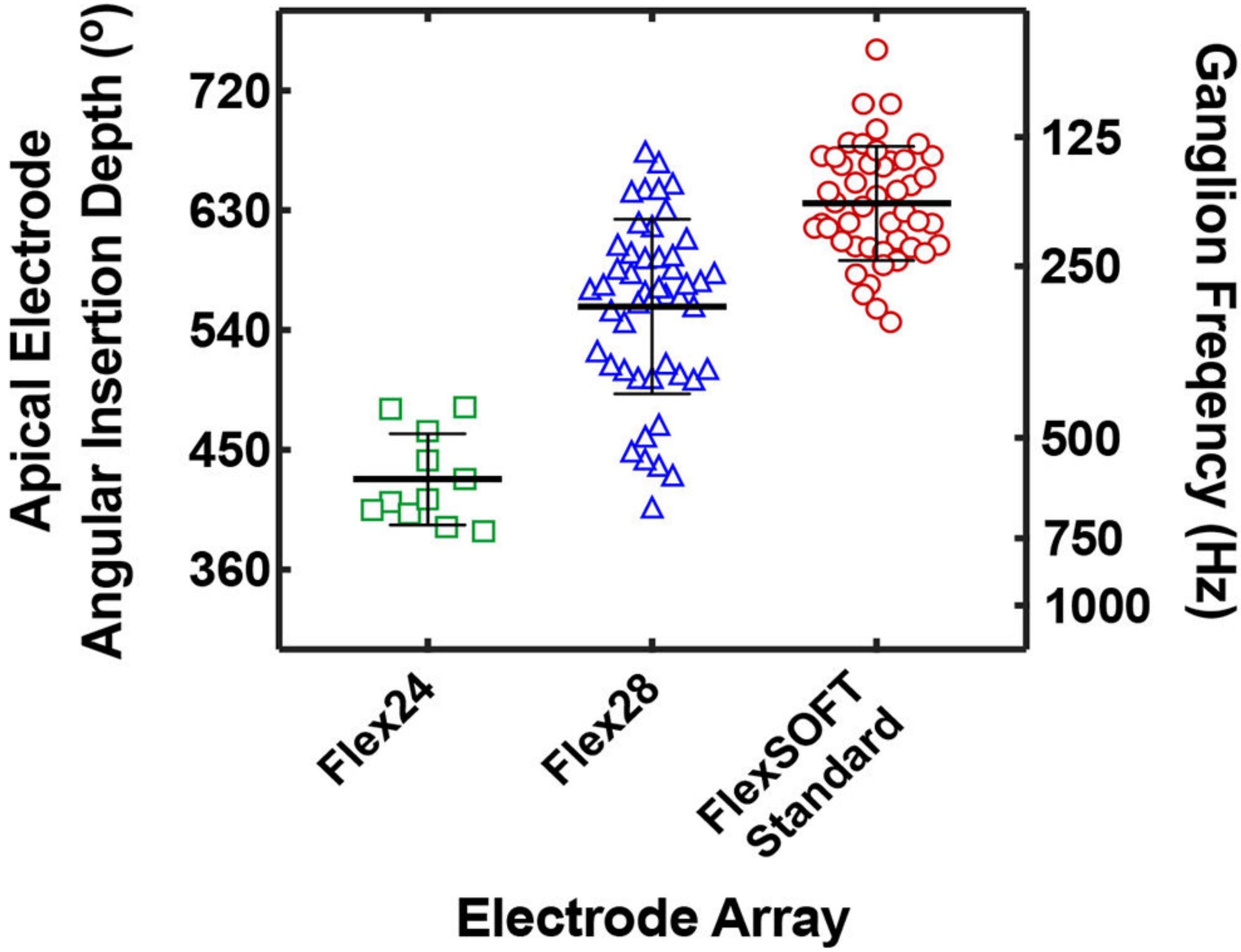

Fig. 1.

Mean angular insertion depth of the most apical electrode contact with standard deviations for complete insertions of Flex24, Flex28, and FlexSOFT/Standard arrays. The predicted cochlear place frequency determined by the spiral ganglion map equation is displayed on the right axis.

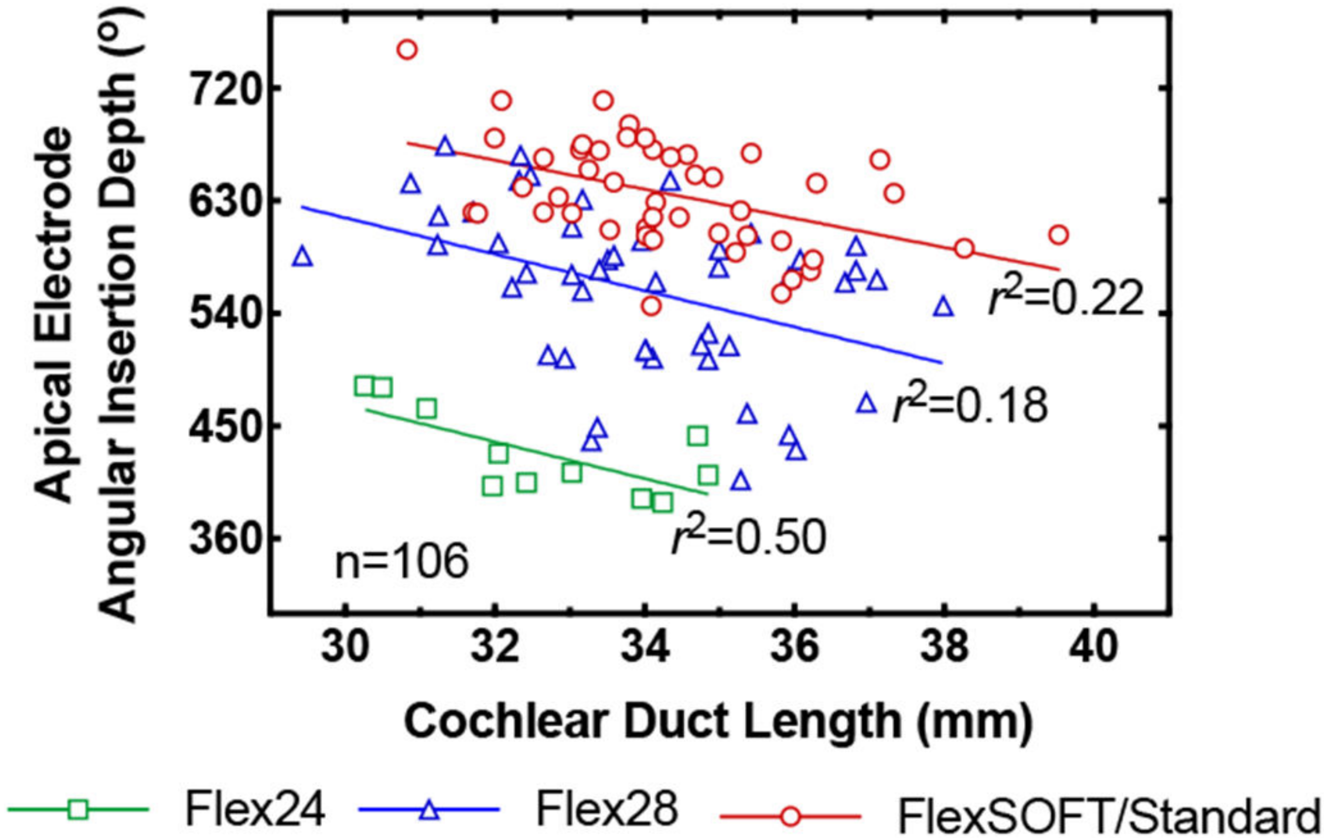

Fig. 2.

Correlation between cochlear duct length and angular insertion depth of the apical electrode contact for complete insertions of Flex24, Flex28, and FlexSOFT/Standard arrays. Electrode array types are shown with different colored shapes as defined in the legend.

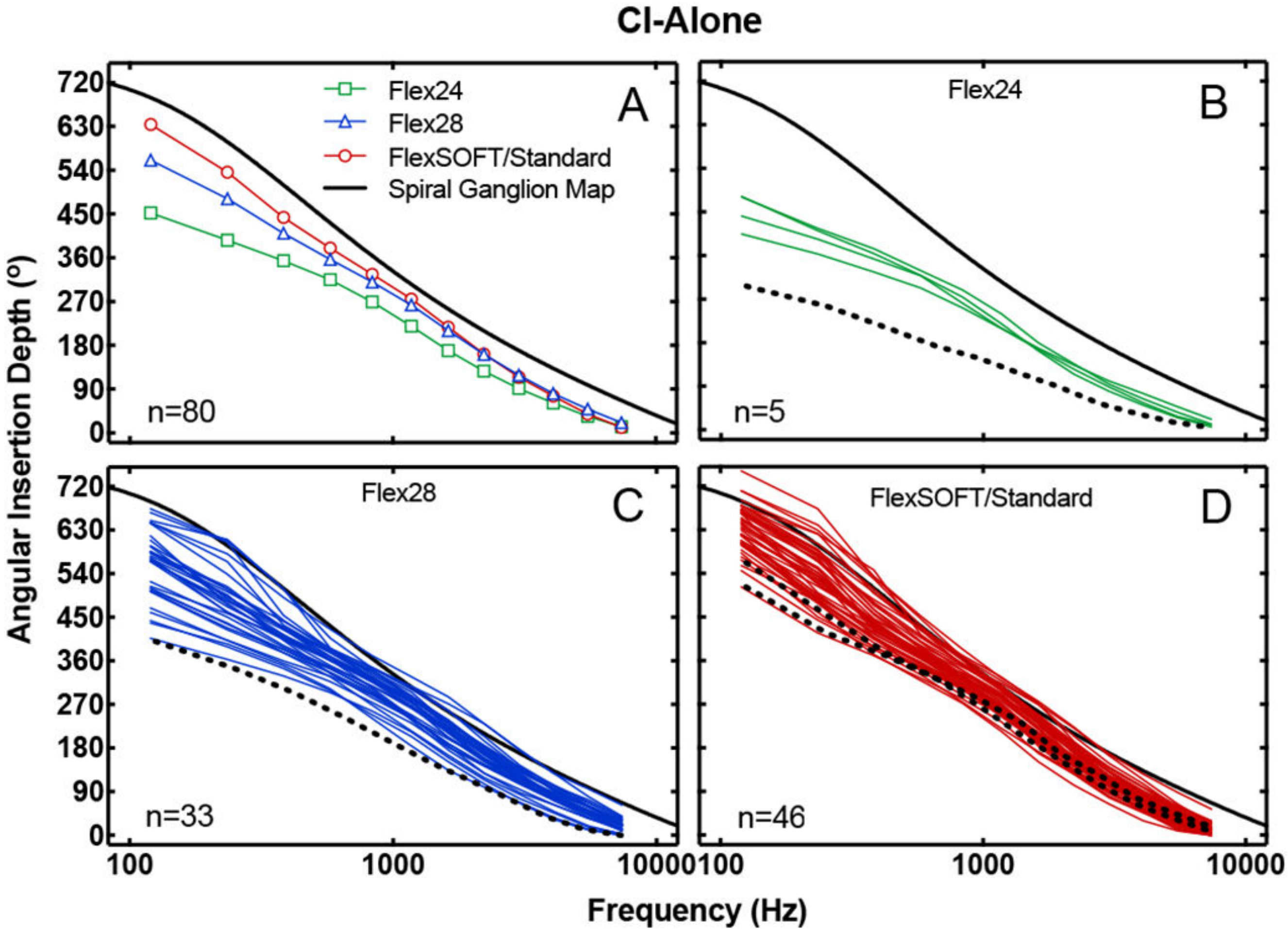

Fig. 3.

(A) Mean angular insertion depth of each electrode contact for complete insertions of Flex24 (green squares), Flex28 (blue triangles), and FlexSOFT/Standard (red circles) arrays as a function of the manufacturer's recommended default center frequency in CI-alone users. Individual differences by electrode array are demonstrated for (B) Flex24, (C) Flex28, and (D) FlexSOFT/Standard arrays. The estimated cochlear place frequency with the spiral ganglion map is represented by the solid black line. Dotted black lines denote data for individuals with partial insertions.

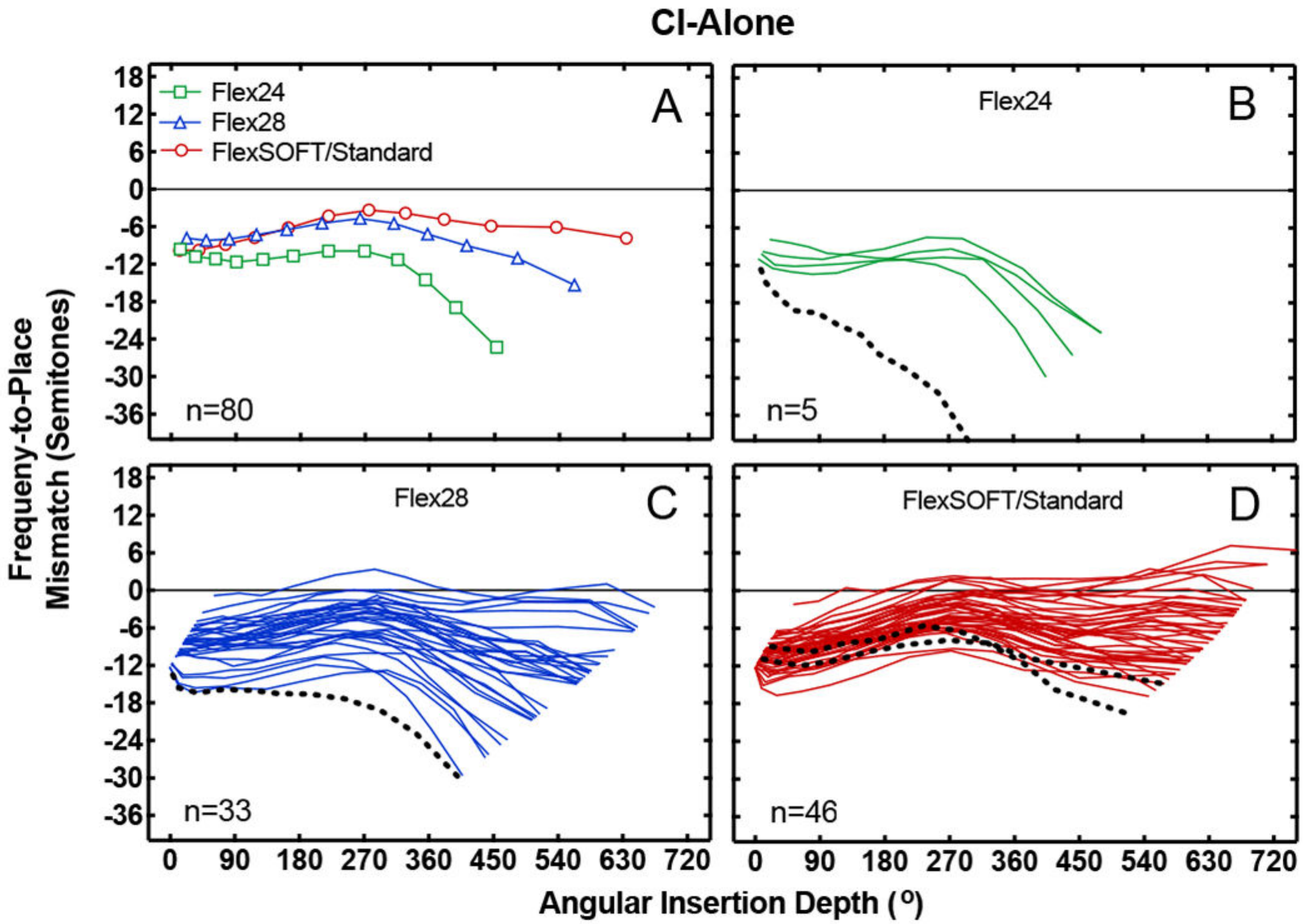

Fig. 4.

(A) Mean frequency-to-place mismatch in CI-alone users with complete insertions and default frequency filters represented by deviation in semitones of the electric place of stimulation from the estimated spiral ganglion frequency, and (B-D) degree of mismatch for individuals implanted with the same array. Dotted black lines denote data for individuals with partial insertions. Electrode array types are shown with different colored shapes as defined in the legend.

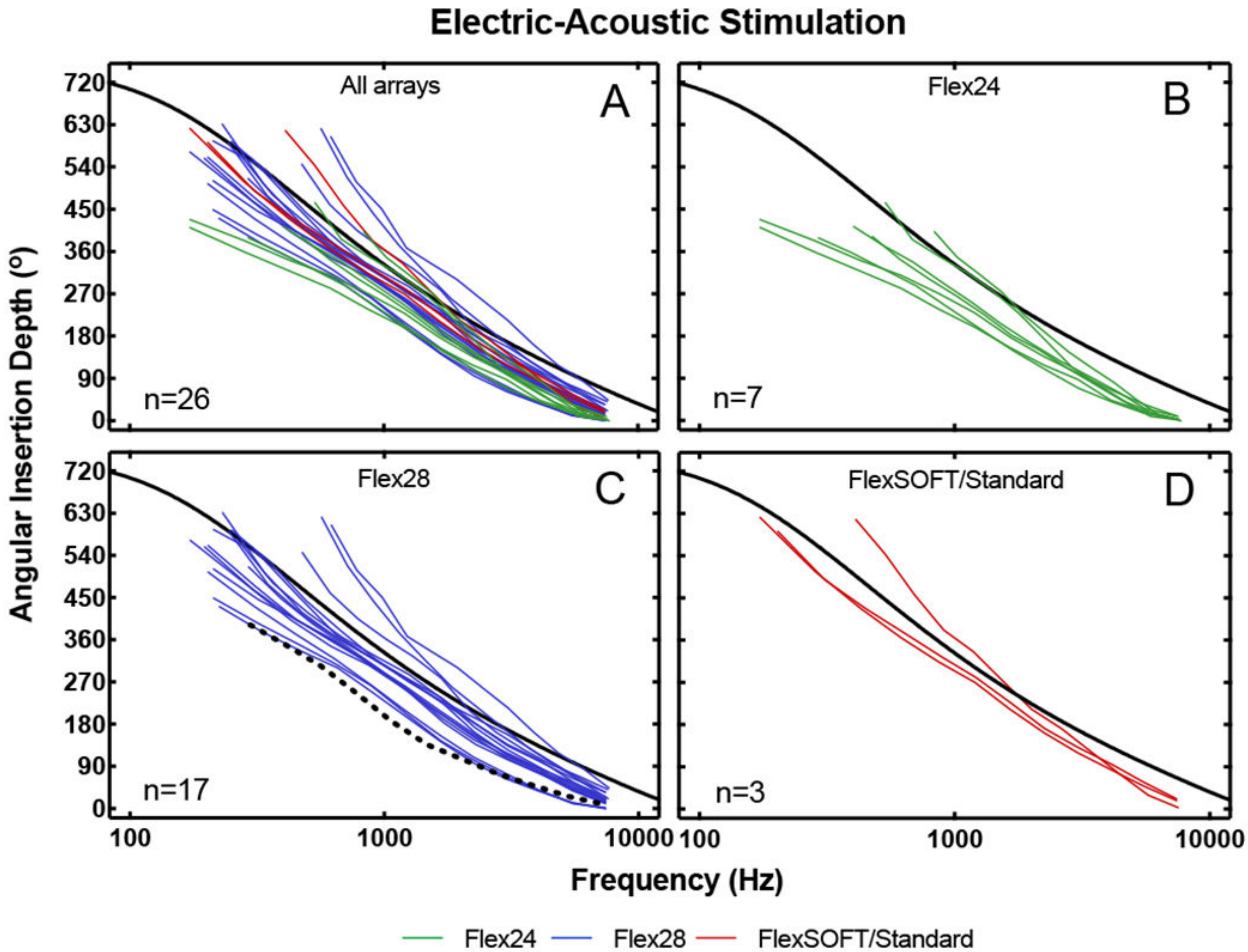

Fig. 5.

(A) Angular insertion depth of each electrode contact as a function of the default electric frequency filters for individual EAS device users with complete insertions and (B-D) data by array type. The estimated spiral ganglion cochlear place frequency is represented by the solid black line. Dotted black lines denote data for individuals with partial insertions.

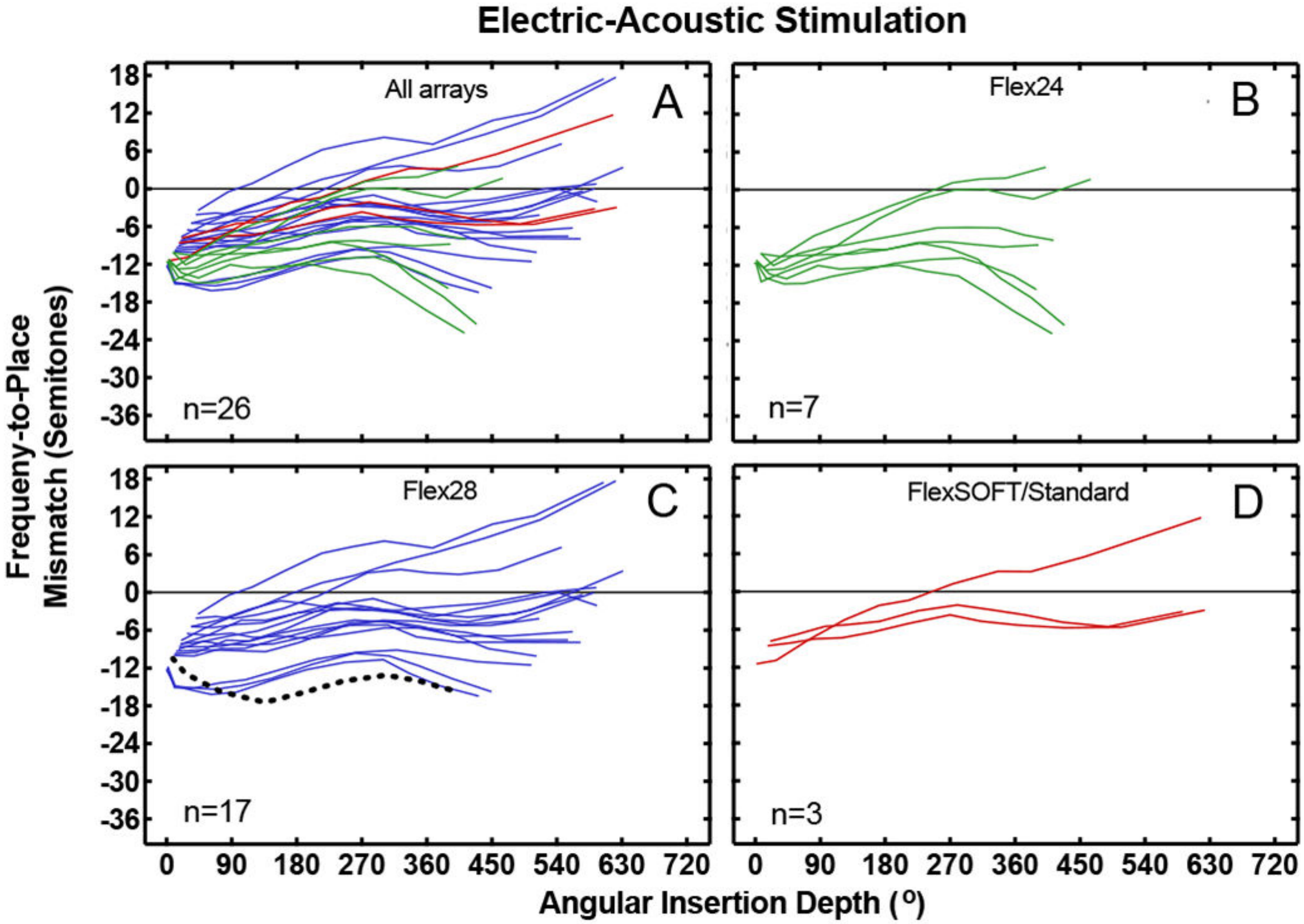

Fig. 6.

(A) Frequency-to-place mismatch in electric-acoustic stimulation device users with default frequency filters, represented by deviation in semitones of the electric place of stimulation from the estimated spiral ganglion frequency and (B-D) additionally separated by array type. Dotted black lines denote data for individuals with partial insertions.

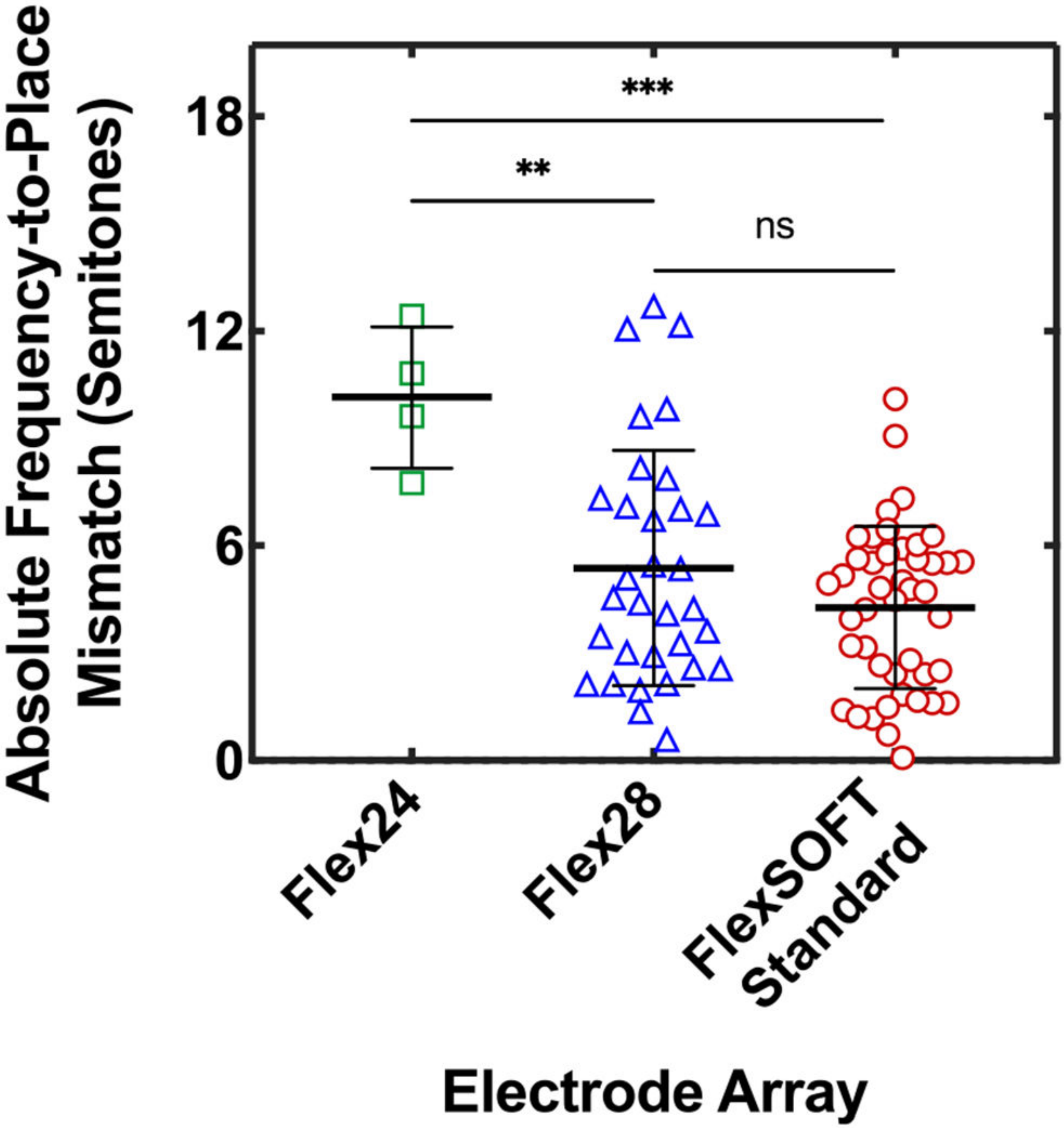

Fig. 7.

Relationship between absolute frequency-to-place mismatch at 1500 Hz (approximate spectral center of important speech information) and array type for CI-alone users with complete insertions. ns, not statistically significant; **, $p < 0.01$; ***, $p < 0.001$.

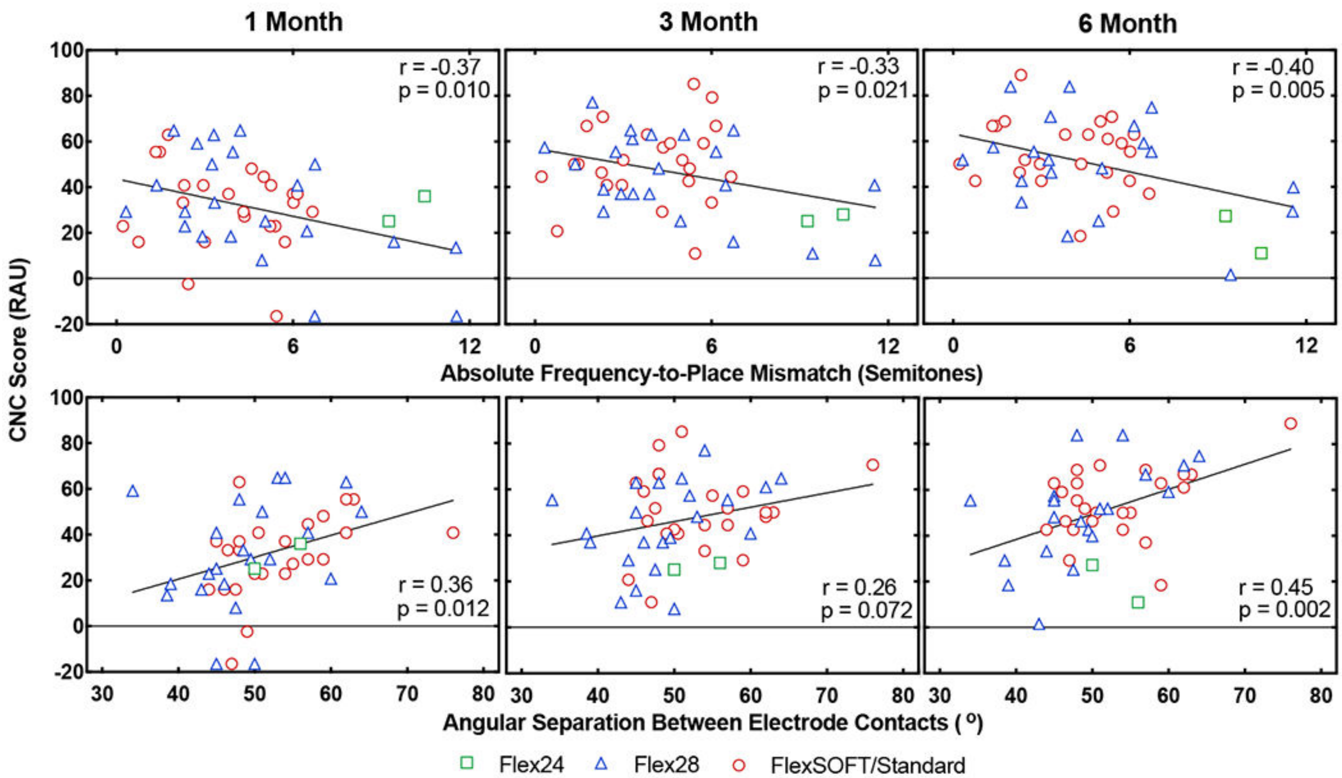

Fig. 8.

CNC word scores in RAU plotted as a function of absolute frequency-to-place mismatch at 1500 Hz (top row), and angular separation between neighboring electrode contacts (bottom row). Data in separate columns indicate results at 1, 3, and 6 months post-activation for CI-alone users with complete insertions ($n = 48$). Symbol color and shape reflects the electrode array type, as defined in the legend. Text at the right of each panel indicates the correlation illustrated with line fits. CNC, consonant-nucleus-consonant; RAU, rationalized arcsine unit.

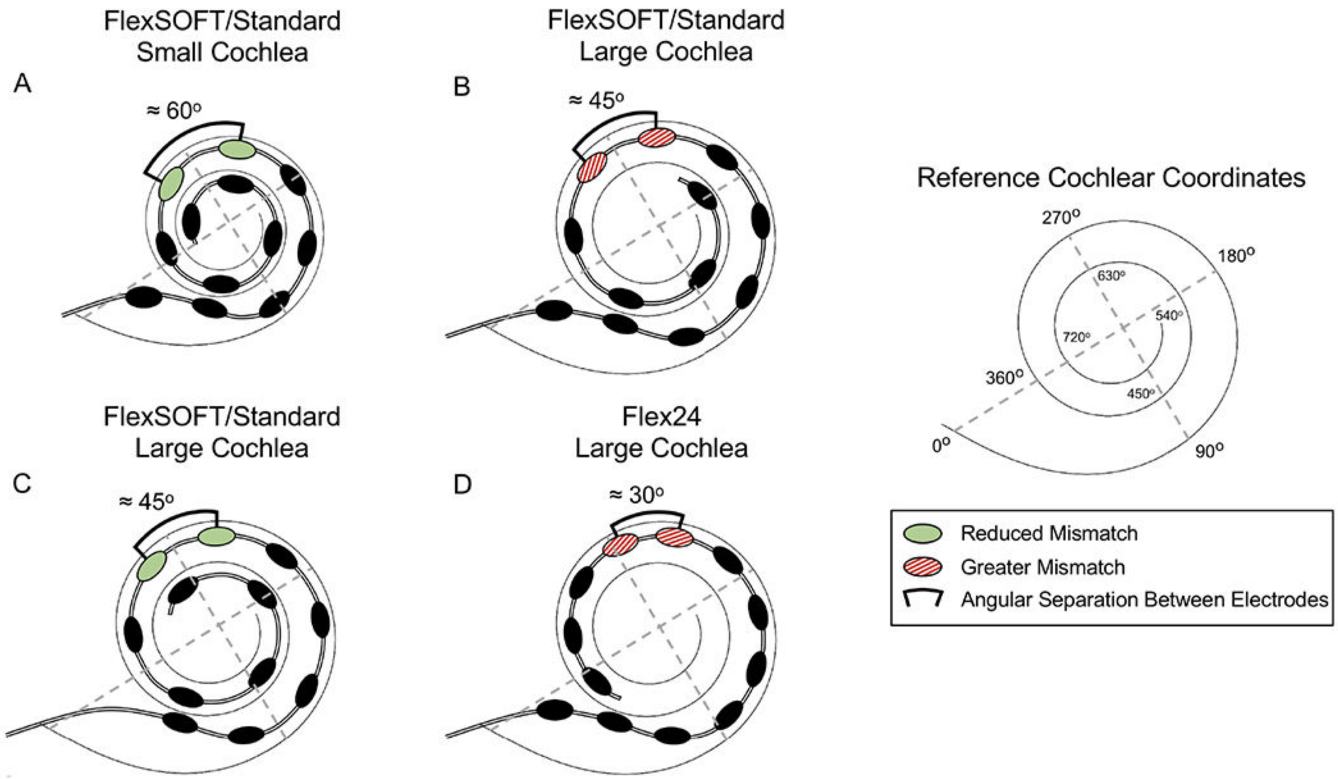

Fig. 9.

Four schematics illustrating the relationship between frequency-to-place mismatch and angular separation between neighboring electrode contacts. Electrode contacts located in the approximate 1-2 kHz region on the spiral ganglion map (224° to 333°) are highlighted in green or red stripes to depict relatively smaller or larger frequency-to-place mismatches, respectively. Cochlear duct length (Panel A vs. B), basal insertion depth (Panel B vs. C), and differences in electrode contact spacing between array types (Panels A-C vs. D) all contribute to varying degrees of both mismatch and angular separation between electrode contacts across individuals.

Author Manuscript

Author Manuscript

Author Manuscript

TABLE 1.

Regression coefficients for a model predicting AID of the most apical electrode with CDL, AID of the most basal electrode, and dummy coding of array type (Flex24 as the default).

	Coef.	SE	t	*p*-value
CDL	−19.27	1.93	−9.99	< 0.001
AID of most basal electrode	3.22	0.31	10.56	< 0.001
Array (FlexSOFT/Standard)	223.80	11.68	19.15	< 0.001
Array (Flex28)	113.90	11.98	9.51	< 0.001

CDL, cochlear duct length; AID, angular insertion depth.

TABLE 2.

Regression coefficients for a model predicting CNC word scores with frequency-to-place mismatch, angular distance between electrode contacts, and test interval (1, 3, 6 months).

	Coef.	SE	t	*p*-value
Mismatch[a]	−2.43	0.52	−4.65	< 0.001
Angular distance[b]	0.75	0.19	3.94	< 0.001
Participant	−0.16	0.10	−1.58	0.117
Test interval	9.70	1.71	5.66	< 0.001

[a]Quantified at 1500 Hz on the spiral ganglion map,

[b]Calculated for electrode contacts located between 1-2 kHz on the spiral ganglion map

TABLE 3.

Relationship between default center frequencies and predicted cochlear place frequency on the spiral ganglion map for participants with complete insertions.

	Mean Angular Insertion Depth (Predicted SG Hz)		
Electrode contact no. (Default center frequency in Hz)	**Flex24 (n=11)**	**Flex28 (n=48)**	**FlexSOFT/ Standard (n=47)**
1 (120)	428 (590)	558 (296)	636 (185)
2 (235)	376 (782)	478 (453)	537 (332)
3 (384)	337 (978)	409 (653)	444 (542)
4 (579)	299 (1225)	355 (880)	381 (761)
5 (836)	255 (1624)	308 (1160)	326 (1041)
6 (1175)	209 (2236)	261 (1560)	275 (1425)
7 (1624)	163 (3177)	208 (2252)	220 (2066)
8 (2222)	122 (4476)	160 (3255)	163 (3177)
9 (3019)	86 (6187)	118 (4635)	116 (4717)
10 (4084)	53 (8479)	81 (6482)	76 (6794)
11 (5507)	25 (11279)	49 (8821)	39 (9752)
12 (7410)	7 (13814)	21 (11775)	12 (13172)

SG, spiral ganglion.

TABLE 4.

Relationship between early speech perception performance and frequency-to-place mismatch provided by each electrode contact.

Electrode contact no.	Correlation between frequency-to-place mismatch and CNC at 6 months (r) (n=48)
1	−0.324 *
2	−0.330 *
3	−0.382 **
4	−0.390 **
5	−0.468 ***
6	−0.389 **
7	−0.257
8	−0.170
9	−0.162
10	−0.158
11	−0.122
12	−0.077

CNC, consonant-nucleus-consonant.

*, $p < 0.05$;

**, $p < 0.01$;

***, $p < 0.001$.